# Raman of Indigo on a Silver Surface. Raman and Theoretical Characterization of Indigo Deposited on a Silicon Dioxide-Coated and Uncoated Silver Nanoparticles

**Article** *in* Spectroscopy Letters · May 2017
DOI: 10.1080/00387010.2017.1324493

CITATIONS
0

READS
160

**5 authors**, including:

Juan-Sebastián Gómez-Jeria
University of Chile
**187** PUBLICATIONS **1,468** CITATIONS
SEE PROFILE

Freddy Celis
Playa Ancha University
**18** PUBLICATIONS **165** CITATIONS
SEE PROFILE

José Javier Cárcamo-Vega
University of Tarapacá
**26** PUBLICATIONS **230** CITATIONS
SEE PROFILE

Taylor & Francis
Taylor & Francis Group

Spectroscopy Letters

An International Journal for Rapid Communication

ISSN: 0038-7010 (Print) 1532-2289 (Online) Journal homepage: http://www.tandfonline.com/loi/lstl20

# Raman of Indigo on a Silver Surface. Raman and Theoretical Characterization of Indigo Deposited on a Silicon Dioxide-Coated and Uncoated Silver Nanoparticles

Guillermo Corales, Freddy Celis, Juan S. Gómez-Jeria, Marcelo Campos & José J. Cárcamo-Vega

**To cite this article:** Guillermo Corales, Freddy Celis, Juan S. Gómez-Jeria, Marcelo Campos & José J. Cárcamo-Vega (2017): Raman of Indigo on a Silver Surface. Raman and Theoretical Characterization of Indigo Deposited on a Silicon Dioxide-Coated and Uncoated Silver Nanoparticles, Spectroscopy Letters

**To link to this article:** http://dx.doi.org/10.1080/00387010.2017.1324493

Accepted author version posted online: 04 May 2017.

# Raman of Indigo on a Silver Surface. Raman and Theoretical Characterization of Indigo Deposited on a Silicon Dioxide-Coated and Uncoated Silver Nanoparticles

Guillermo Corales[1], Freddy Celis[2], Juan S. Gómez-Jeria[3], Marcelo Campos[3], José J. Cárcamo-Vega[1,4]

[1]Departamento de Química, Facultad de Ciencia, Universidad de Tarapacá, Arica, Chile [2]Departamento de Química y Centro de Estudios Avanzados, Universidad de Playa Ancha, Valparaíso, Chile [3]Laboratorio de Espectroscopía Vibracional, Facultad de Ciencias, Universidad de Chile, Santiago, Chile [4]Laboratorio de Análisis e Investigaciones Arqueométricas (LAIA), Instituto de alta Investigación (IAI), Universidad de Tarapacá, Arica, Chile

Corresponding author J. Cárcamo-Vega , E-mail: jcarcamo@uta.cl / jjcarcamo@gmail.com



## Abstract

Raman, surface enhanced Raman scattering and shell isolated nanoparticles enhanced Raman scattering techniques were used to study the indigo/nanoparticle interaction nature. Silver nanoparticles were employed with and without a silicon dioxide spacer inert layer. The surface enhanced Raman scattering spectral profile, obtained by using silver nanoparticles, is different than the Raman one which allowed propose that the indigo/silver interaction is in the range of the intermolecular interactions. Surface enhanced Raman scattering spectral reproducibility suggests identical organization and orientation of the analyte on the metal surface. The shell isolated nanoparticles enhanced Raman scattering spectrum, obtained by using silicon dioxide coated silver nanoparticles resulted similar to the Raman. This result indicates that the indigo structure is chemically unmodified by the silicon dioxide coated silver surface. From the shell isolated nanoparticles enhanced Raman scattering experiments the electromagnetic mechanism is proposed as being the unique contribution to the spectral enhancement. Theoretical

calculations allow infer about both the indigo/silver surface interaction nature and on the orientation of indigo on the surface.

**KEYWORDS:** Indigo, Raman, SERS, SHINERS, Silicon Dioxide Coated Silver Nanoparticles

## INTRODUCTION

The present work deals with the characterization of the indigo silver-metal interaction by using Raman scattering, Surface Enhanced Raman Scattering (SERS) and Shell-Isolated Nanoparticles Enhanced Raman Scattering (SHINERS) spectroscopies. These techniques have become important analytical tools to study pigments and dyes. Raman spectroscopy is recognized to be a powerful technique to analyze archaeological objects [1–9]. It is a non-invasive and non-destructive technique, displaying high specificity, sensitivity and reproducibility [10,11]. Concerning SERS, there is a consensus that the amplification of the vibrational signals is due to electromagnetic (EM) and chemical (QM) mechanisms [12]. The first arises mainly from the coupling of light with the plasmons on the metal surface, driving its subsequent excitation. The QM mechanism is originated by charge transfer between the analyte molecules and the metal substrate which has a low enhancement factor of $10\text{-}10^{-2}$ [13].

Recently, a new technique has been developed to obtain enhanced Raman spectra by using silicon dioxide ($SiO_2$) coated nanoparticles (SHINs, shell-isolated nanoparticles). $SiO_2$ coating requires successive hydrolysis-condensation cycles [14–16]. Only the

electromagnetic mechanism is involved in the Raman signal enhancement of the SHINERS technique [16–18]. The signal intensity is modulated by the thickness of the inert layer on the surface of the nanoparticle. For example, it has been reported that for 55 nm of gold particles (NPs) 2 nm of $SiO_2$ are formed at 20 min (1 h = 4 nm, 2 h = 6 nm, 4 h = 8 nm, 8 h =10 nm and 20 h = 20 nm) [16]. The reaction rate depends on the pH value. An advantage of the SHINs synthesis is the opportunity to dry, wash and reuse the nanomaterial. Applications of SHINs have been described in surface science, electrochemistry, semiconductor materials, biological science and food science [19].

The present contribution intends to give some structural insights about the interaction of the indigo molecule (see Fig. 1) with $SiO_2$ uncoated and coated silver nanoparticles (Ag@$SiO_2$NPs, core@shell) by using the Raman, SERS and SHINERS techniques, and consequently infer about the interaction mechanisms. A theoretical interpretation of the metal-molecule interaction based on simplified molecular models is also performed.

## EXPERIMENTAL

### *Materials*

Indigo (95% purity) in solid, see Fig. 1, was purchased from Sigma-Aldrich. The following chemicals were used for the preparation of the colloidal solutions of silver nanoparticles: silver nitrate 99.9999% metal basis (Aldrich), sodium hydroxide (ACS, Reag. Ph Eur Merck) and sodium citrate tribasic dihydrate ≥99.0% Sigma-Aldrich. 3-aminopropyltrimethoxysilane and sodium silicate solution were purchased from Sigma-Aldrich. All these chemicals were used as received.

***Synthesis Of The Silver And Silicon Dioxide Coated Silver Nanoparticles***

Silver colloidal nanoparticles (AgNPs) were prepared following a previously reported procedure [20,21]. Briefly, the hydroxylamine hydrochloride-reduced colloid was prepared by adding 10 mL of silver nitrate ($10^{-2}$ M) to a 90 mL of hydroxylamine hydrochloride ($10^{-3}$ M) and sodium hydroxide ($10^{-3}$ M) solutions. The AgNps were obtained at room temperature under rapid stirring conditions. Ag@$SiO_2$NPs were obtained following a reported pathway [19,22], as follows: to 30 mL of AgNps 0,4 mL of (3-aminopropyl)trimethoxysilane $10^{-3}$ M was added and stirred during 15 minutes. Then, 3.2 mL of silicate solution (pH=10) was added, stirring and heating at 90°C. After 20 minutes of synthesis (for a thickness of 2 nm of the $SiO_2$ coating) the nanoparticles were cleaned and concentrated by centrifugation (5 minutes at 5000 rpm thrice). The AgNps and Ag@$SiO_2$NPs characterization was carried out with UV-vis spectra and scanning electron microscopy (SEM).

***UV-Vis Spectrum Of Silver And Silicon Dioxide Coated Silver Nanoparticles***

The UV-vis spectra of AgNPs and Ag@$SiO_2$NPs in Fig. 2, were obtained from 200 uL of each colloidal system which were dissolved in 0.8 mL of ultrapure water. Spectra were scanned between 350 and 700 nm by using 1 cm optical path quartz cells and a Genesys 6 spectrophotometer; the spectral resolution is 1.8 nm. Maxima are observed at 407 and 420 nm for AgNPs and Ag@$SiO_2$NPs, respectively (Fig. 2). This red shift is associated to the effect that the $SiO_2$ shell has on the silver nanoparticles; the slight shifting indicates

that the effect of the shell on the localized surface plasmon resonances (LSPR) is negligible [17].

***Scanning Electron Microscopy Measurements Of Silver Nanoparticles And Silicon Dioxide Coated Silver Nanoparticles***

For the Scanning Electron Microscopy (SEM) measurements, samples of AgNPs dispersed in methanol were deposited onto carbon-coated copper grids. A JEOL JSM-7500F field-emission scanning electron microscope equipped with a Transmission Electron Detector (TED) was used to obtain low-resolution transmission images of the Ag@$SiO_2$NPs nanoparticles. The $SiO_2$ coating onto the silver nanoparticle is observed in the SEM image in Fig. 3; the nanoparticles size is in the range of 100-150 nm. A "cradle-of-hotspots" that is $SiO_2$ glued nanoparticles also results from the core@shell synthesis [22].

***Sample Preparation For The Spectral Measurements***

Indigo solution was prepared from the solid dissolved in acetone to a final concentration of $10^{-5}$ M. Then, 100 μL of this solution was added to 400 μL of each colloidal Ag and Ag@$SiO_2$NPs solutions. Resulting mixtures rest for 24 hrs. These mixtures were centrifuged for 3 min with a maximum speed of 7000 rpm (2.1G) and the obtained solids were then deposited on a slide where remained solvent was evaporated at room temperature.

***Micro-Raman Measurements***

Micro-Raman spectra of the samples were recorded with a Raman Renishaw InVia Reflex apparatus, equipped with the 532, 633, and 785 nm laser lines, a Leica microscope and an electrically cooled CCD detector. The instrument was calibrated using the 520 $cm^{-1}$ line of a Si wafer and a 50× objective. Its resolution was set to 4 $cm^{-1}$ and 1-20 scans of 10-30 s each were averaged. Spectra were recorded in the 300-1800 $cm^{-1}$ region. The laser power was set between 10 to 100 mW. Spectral scanning conditions were chosen to avoid sample degradation and photodecomposition; the 532 nm laser line was used. Data were collected and plotted using the programs WIRE 3.4 and GRAMS 9.0. Raman, SERS and SHINERS spectra are displayed in Fig. 4.

***Theoretical Analysis***

A model for the metal surface was built as in our previous studies [23,24]. A face centered-cubic structure with d(Ag-Ag)= 4.08 Å was cropped to get a planar bilayer composed of 800 Ag atoms. Extended Hückel Theory (EHT) calculations of the electronic structure of neutral indigo were complemented with DFT at the B3LYP/6-31G(d,p) level for comparison. The last method was also employed to calculate the infrared and Raman spectra of neutral indigo. EHT produces qualitative or semi quantitative descriptions of the molecular orbitals and electronic properties [25]. Moreover, and within the Hartree-Fock-Rüdenberg picture, EHT is compatible with the nonempirical HF method in Roothaan's form [26]. This methodology was discussed and applied in our previous papers [27–29]. HyperChem (Hypercube, Inc.) and Gaussian (Version 09, Revision A.1. Gaussian, Inc., Wallingford, CT) programs were employed for calculations. Molecular mechanics at the OPLS level was used to optimize the indigo–Ag geometry, keeping the Ag layer

geometry fixed. The molecules were positioned at several different distances and orientations from the center of the Ag layer. The aim of this simplified system is to correlate the enhanced bands in the SERS spectrum with the molecule's affinity towards the Ag surface. This direct interaction occurs when thermal agitation carries out the molecules relatively near to the surface with no solvent molecules between them. This situation agrees with one of the necessary conditions to obtain a SERS spectrum (the other is that the molecule-surface interaction must occur on a hot spot). It is worth to mention that the calculations, their analysis and the predictions were made prior to the knowledge of the SERS measurements. This method was successfully employed in our previous SERS studies for the interaction of peptides, nanotubes, tryptophan, lysine, humic acids, proline, with Ag and Au surfaces [30-33].

## RESULTS AND DISCUSSION

### *Raman Spectrum*

The present bands assignment of solid indigo in Table 1 is proposed on the basis of general data [34-36] and from published vibrational spectra of related and close molecular systems [37,38]. The most intense signal of the ring stretching mode is observed at 1573 $cm^{-1}$ with a shoulder at 1591 $cm^{-1}$ due to the νC=C, νC=O and in plane NH deformations (δNH) modes, see Fig. 4A. The bands at 1702, 1631 and 1365 $cm^{-1}$ are due to νCC, νC=O and δNH coupled modes of the heterocyclic structural fragment. The bands at 1311 and about 860 $cm^{-1}$, are attributed to coupled vibrations involving the stretching and bending vibrations of the six-member ring, which is supported by the theoretical data. A δCH mode is in principle assigned to the weak band observed at 1147 $cm^{-1}$. According to

the present calculations this band results from coupled δCH and breathing modes. The band at 1225 $cm^{-1}$ is assigned to a bending mode involving the N–H bond. Bands at 1483, 1461 and 1248 $cm^{-1}$ are ascribed to C–H deformations. The calculations allowed assign the bands at 1015, 758 and 674 $cm^{-1}$ to the five- and six-member ring vibrations. The broad band at 635 $cm^{-1}$ is probably due to skeletal vibrations involving the NCC moiety. The medium band at 598 $cm^{-1}$ is a NH deformation while the strong band at 545 $cm^{-1}$ is an out of plane CH deformation (ρCH). Vibrations related to the CNC structural fragment are expected below 500 $cm^{-1}$.

***Surface Enhanced Raman Scattering Spectrum***

Identical SERS spectra of indigo originally prepared at different concentrations ($10^{-4}$ M to $10^{-7}$ M) were obtained. Relative to the Raman spectrum various spectral modifications are observed by surface effect, see Fig. 4B. In fact, the strongest band at 1573 $cm^{-1}$ with a shoulder at highest numbers shifts to 1564 $cm^{-1}$ displaying a slight asymmetry to highest wavenumbers in the SERS spectrum; a decreasing in the relative intensity is also verified. The wavenumber shift is associated to an electronic redistribution involving the C6C8CO (C10C13CO) and C5C8NH (C10C14NH) structural fragments while the intensity decreasing could be due to a rather tilted position of this fragment on the surface. This orientation is proposed on the basis of the SERS selection rules [39]. Thus, the orientation of the analyte is inferred from the observed intensity and wavenumber shifts relative to the Raman spectrum; modes having their $\alpha_{zz}$ component of the polarizability perpendicular to the surface are likely to become more enhanced than the parallel ones. The strong ρCH band at 545 $cm^{-1}$ is enhanced by surface effect and it is observed shifted

to 557 $cm^{-1}$ in the SERS spectrum; this spectral behavior is consistent with a planar parallel orientation of the corresponding CH moiety. The spectral shifting suggests a molecule surface interaction in the range of the intermolecular interactions. The medium band at 598 $cm^{-1}$ ascribed to a NH deformation "probably an out of plane deformation" is not observed in the SERS spectrum which supports the idea that the NH fragment is not parallel to the surface. The weak bands observed only in the SERS spectrum at about 500, 460 and 401 $cm^{-1}$ could be ascribed to out of plane vibrations of the rings oriented parallel to the surface; this spectral assignment is supported by general data [34–36]. The broad Raman band at 635 $cm^{-1}$ shifts to 651 $cm^{-1}$ in the SERS spectrum keeping a similar relative intensity; this is highly consistent with the fact that the NCC moiety is tilted to the surface and that the interaction with the surface involves the N atom. The Raman bands at 674 and 758 $cm^{-1}$ are not observed in SERS which indicates that the corresponding ring modes are vibrating parallel to the surface. By assuming that the rings are rather parallel to the surface and that the C6C8CO and C5C8NH structural fragments are not coplanar into the whole indigo molecule, the ring vibration at 1015 $cm^{-1}$, displaying an increasing of its relative intensity and a shift to 1018 $cm^{-1}$ by surface effect, is an out of plane vibration probably a ρCH mode [34]. The band at 1147 $cm^{-1}$ increases the relative intensity by surface effect; this band is decidedly ascribed to a five-member ring breathing [35]. The observed spectral modification is consistent with a ring oriented nearly parallel to the surface which is supported by the SERS selection rules [39]. The breathing mode of an aromatic ring consists into contract and relaxing all C-C bonds, simultaneously. Then, the up-down oscillation of the electrons cloud perpendicular to the ring plane is associated to the breathing mode having the $\alpha_{zz}$ component of the

polarizability parallel to the incident laser line. An opposite spectral behavior is observed for the bands at 1225, 1311, 1365 and 1461 $cm^{-1}$ which is consistent with spectral modes vibrating not perpendicular to the surface; the fact that the band at 1225 $cm^{-1}$ is still observed in SERS at 1194 $cm^{-1}$ although with a very weak relative intensity could be related to a ring mode belonging to a tilted structural fragment, the C6C8CO and C5C8NH moieties. The above results allow to propose that the indigo molecule interacts with the Ag surface and that this interaction induces some electronic redistribution on the molecule. Moreover, the indigo molecule is oriented parallel to the surface as a whole, but the CO and NH fragments are not exactly parallel to the surface.

***Shell-Isolated Nanoparticles Enhanced Raman Scattering Spectrum***

A Raman enhancement effect, Fig. 4C, is observed from the spectra obtained by using $SiO_2$ coated Ag nanoparticles and indigo originally prepared at two concentrations ($10^{-5}$ M and $10^{-7}$ M); SHINERS spectra obtained from both concentrations resulted identical. The SHINERS spectrum arises from "cradle of hot-spots" originated from the synthesis of the shell-isolated nanoparticles (Fig. 3). The term “cradle of hot-spots” is introduced to describe the physical aspect of the resulting coated nanoparticles. This arrangement of the nanoparticles is a direct consequence of the aggregation during the synthesis as described by Aroca et al. [40] and by us in a previous work [22].

The $SiO_2$ coating of the Ag colloids guarantees a non-chemical binding or bonding between the indigo molecule and the metal surface. As a consequence it is expected that the SHINERS and Raman spectral profiles should not be quite different, as observed in

Fig. 4A and 4C. This result indicates that the indigo Ag interaction inferred from the SERS spectrum involves a chemical contribution to the Raman signals enhancement. The fact that the Raman signals of the analyte at very low concentration are still observed in SHINERS indicates that the enhancement is now arising from an electromagnetic or physics mechanism; the indigo structure is not modified by the surface.

***Theoretical Data***

The final geometry of the indigo-Ag surface is shown in Fig. 5. The most important fact to notice is that the carbonyl oxygen and the hydrogen atoms bonded to the nitrogen moved a little away from the molecular plane. The H atoms bonded to N atoms move away from indigo's plane and the Ag surface, while the carbonyl oxygen also moves away from the molecular plane but toward the Ag surface. Each oxygen atom is engaged in two metal interactions with metal cations (the Ag atoms have positive net charge in our Ag surface model, since the HOMO is not localized in the center of the surface) and hydrogen bond. These distances are in the range of 3.17-3.32 Å. The slight molecular deformation seems to be an indication of a strong electrostatic molecule-surface interaction.

## CONCLUSIONS

The Raman spectroscopy and the SERS and SHINERS techniques were used to infer about the chemical physics nature of the indigo Ag surface interaction. The SERS spectral profile is different from the Raman spectrum which allowed to propose that the indigo Ag interaction is in the range of the intermolecular interactions. Vibrations

involving the N and O atoms structural moieties are sensitive to the Ag surface effect. The SERS spectral reproducibility suggests identical batch to batch organization and orientation of the analyte on the metal surface. The SHINERS spectra resulted identical at various concentrations of the analyte and very close to the Raman spectrum. Thus, only a physical contribution on the spectral enhancement of the SHINERS spectrum is inferred. These differences between SERS and SHINERS are ascribed to structural modifications imposed by the analyte/uncoated Ag metal surface interaction. The whole results indicate that the indigo structure is chemically modified in the SERS experiments. Thus, the enhancement chemical mechanism contributes to the whole SERS effect. The theoretical calculations data are consistent with the SERS experiments and allowed to corroborate that the indigo metal interaction involves the oxygen and nitrogen atoms. From this study, we can infer a rather plane parallel orientation of the analyte to the surface.

## ACKNOWLEDGEMENTS

This work was financially supported by projects 11140262 and 1140524 from FONDECYT. FCB acknowledge to postdoctoral project 3150222 from FONDECYT.

## REFERENCES

1. Tian W., Zhu T., Brunet M., Deshayes C., and Sciau P. Raman study of Yuan Qinghua porcelain: the highlighting of dendritic $CoFe_2O_4$ crystals in blue decorations. *J. Raman Spectrosc.* **2017**, 48(2), 267-270.

2. Łydżba-Kopczyńska B. and Madariaga J. M. Applications of Raman spectroscopy in art and archaeology. *J. Raman Spectrosc.* **2016**, 47(12), 1404–1407.

3. Coccato A., Bersani D., Coudray A., Sanyova J., Moens L. and Vandenabeele P. Raman spectroscopy of green minerals and reaction products with an application in Cultural Heritage research. *J. Raman Spectrosc.* **2016**, 47(12), 1429–1443.

4. Hernanz A., Iriarte M., Bueno-Ramírez P., de Balbín-Behrmann R., Gavira-Vallejo J.M., Calderón-Saturio D., Laporte L., Barroso-Bermejo R., Gouezin Ph., Maroto-Valiente A., Salanova L., Benetau-Douillard G. and Mens E., Raman microscopy of prehistoric paintings in French megalithic monuments. *J. Raman Spectrosc*., **2016**, 47(5), 571–578.

5. Zaffino Ch., Dulcedo Bedini G., Mazzola G., Guglielmi V. and Bruni S. Online coupling of high-performance liquid chromatography with surface-enhanced Raman spectroscopy for the identification of historical dyes. *J. Raman Spectrosc.* **2016**, 47(5), 607–615.

6. Pozzi F. and Leona M. Surface-enhanced Raman spectroscopy in art and archaeology, *J. Raman Spectrosc*., **2016**, 47(1),67–77.

7. Sepúlveda M., Gutiérrez S., Campos- Vallette M.M., Clavijo R.E., Walter P. and Cárcamo J.J., Raman Spectroscopy and X-ray fluorescence in molecular analysis of yellow blocks from the archeological site Playa Miller 7 (northern Chile), *J. Chil. Chem. Soc*., **2013**, 58(3), 1836-1839.

8. Lahlil S., Lebon M., Beck L., Rousselière H., Vignaud C., Reiche I., Menu M., Paillet P. and Plassard F., The first *in situ* micro-Raman spectroscopic analysis of prehistoric cave art of Rouffignac St-Cernin, France. *J. Raman Spectrosc.*, **2012**, 43(11), 1637-1643.

9. Casanova- González E., García- Bucio A., Ruvalcaba- Sil J.L., Santos- Vasquez V., Esquivel B., Falcón T., Arroyo E., Zetina S., Roldán M.L. and Domingo C. Surface-enhanced Raman spectroscopy spectra of Mexican dyestuffs. *J. Raman Spectrosc*., **2012**, 43(11), 1551-1559.

10. Colomban, P. and Treppoz, F. Identification and differentiation of ancient and modern European porcelains by Raman macro- and micro-spectroscopy. *J. Raman Spectrosc*. 2001, 32(2), 93-102.

11. Boucherit N., Goff A.H. and Joiret S. Raman studies of corrosion films grown on Fe and Fe-6Mo in pitting conditions. *Corros. Sci*. **1991**, 32 (5-6) 497-507.

12. Kambhampati P., Child C.M., Foster M.C. and Campion A. On the chemical mechanism of surface enhanced Raman scattering: Experiment and theory. *J. Chem. Phys*. **1998**, 108, 5013-5026.

13. Aroca R., Chemical Effects and the SERS Spectrum. In *Surface-Enhanced Vibrational Spectroscopy*, John Wiley & Sons, Ltd: Chichester, 2006, 107-132.

14. Zhang B.Q., Li S.B., Xiao Q., Li J. and Sun J.J. Rapid synthesis and characterization of ultra-thin shell Au@$SiO_2$ nanorods with tunable SPR for shell-isolated nanoparticle-enhanced Raman spectroscopy (SHINERS). *J. Raman Spectrosc.* **2013**, 44(8), 1120-1125.

15. Shanthil M., Thomas R., Swathi R. S., and Thomas K. G. Ag@$SiO_2$ Core–Shell Nanostructures: Distance-Dependent Plasmon Coupling and SERS Investigation., *J. Phys. Chem. Lett.*, **2012**, 3(11), 1459–1464

16. Zhang K., Qing J., Gao H., Ji J., and Liu B. Coupling shell-isolated nanoparticle enhanced Raman spectroscopy with paper chromatography for multi-components on-site analysis. *Talanta* **2017**, 162, 52–56.

17. Li J.F., Huang Y.F., Ding Y., Yang Z.L., Li S.B., Zhou X.S., Fan F.R., Zhang W., Zhou Z.Y. and Ren B. Shell-isolated nanoparticle-enhanced Raman spectroscopy. *Nature* **2010**, 464(7287), 392-495.

18. Tian X.D., Liu B.J., Li J.F., Yang Z.L., Ren B. and Tian Z.Q. SHINERS and plasmonic properties of Au Core $SiO_2$ shell nanoparticles with optimal core size and shell thickness. *J. Raman Spectrosc*. 2013, 44(7), 994-998.

19. Li J.F., Tian X.D., Li S.B., Anema J.R., Yang Z.L., Ding Y., Wu Y.F., Zeng Y.M., Chen Q.Z., Ren B., Wang Z.L. and Tian Z.Q. Surface analysis using shell-isolated nanoparticle-enhanced Raman spectroscopy. *Nature Protocols* **2013**, 8(1), 52-65.

20. Leopold N. and Lendl B. A New Method for Fast Preparation of Highly Surface-Enhanced Raman Scattering (SERS) Active Silver Colloids at Room Temperature by Reduction of Silver Nitrate with Hydroxylamine Hydrochloride. *J. Phys. Chem. B* **2003**, 107(24), 5723-5727.

21. Diaz Fleming G., Finnerty J.J., Campos-Vallette M., Célis F., Aliaga A.E., Fredes C. and Koch R. Experimental and theoretical Raman and surface-enhanced Raman scattering study of cysteine. *J. Raman Spectrosc.* **2009**, 40(6), 632-638.

22. Celis F., Campos-Vallette M.M., Cárcamo-Vega J., Gómez-Jeria J.S. and Aliaga C. Raman and Surface Enhanced Raman signals of the sensor 1-(4-mercaptophenyl)-2,4,6-triphenylpyridinium perchlorate. *J. Chil. Chem. Soc*. **2015**, 60(2), 2944-2948.

23. Leyton P., Gómez-Jeria J.S., Sanchez-Cortes S., Domingo C. and Campos-Vallette M.M. Carbon Nanotube Bundles as Molecular Assemblies for the Detection of Polycyclic Aromatic Hydrocarbons: Surface-Enhanced Resonance Raman Spectroscopy and Theoretical Studies. *J. Phys. Chem. B* **2006**, 110(13), 6470-6474.

24. Vera A.M., Cárcamo J.J., Clavijo E., Gómez-Jeria J.S., Kogan Bocian M.J. and Campos-Vallette M.M. Interaction of the CLPFFD peptide with gold nanospheres. A Raman, surface enhanced Raman scattering and theoretical study. *Spectrochim. Acta A* **2015**, 134, 251-256.

25. Koch W. On Rüdenberg's integral approximations and their unrestricted and combined use in molecular orbital theories of Hartree–Fock type. *Int. J. Quantum Chem*., **2000**, 76, 148-160.

26. Koch, W., Frey, B., Ruiza, J.F.S., and Scior, T.. On the Restricted and Combined Use of Rüdenberg's Approximations in Molecular Orbital Theories of Hartree-Fock Type. *Zeitschrift für Naturforschung A*, **2003,** 58, 756-784.

27. Garrido C., Aliaga A.E., Gómez-Jeria J.S., Cárcamo J.J., Clavijo E. and Campos-Vallette M.M. Interaction of the C-terminal peptide from pigeon cytochrome C with silver nanoparticles. A Raman, SERS and theoretical study. *Vib. Spectrosc*. **2012**, 61, 94-98.

28. Cárcamo J.J., Aliaga A.E., Clavijo E., Garrido Leiva C., Gómez-Jeria J.S. and Campos-Vallette M.M. Proline and hydroxyproline deposited on silver nanoparticles. A Raman, SERS and theoretical study. *J. Raman Spectrosc*. **2012**, 43(6), 750-755.

29. Muñoz-Pérez J., Leyton P., Paipa C., Soto-Galdamez J.P., Gómez-Jeria J.S. and Campos-Vallette M.M. Raman and surface enhanced Raman scattering study of the

orientation of cruciform 9,10-anthracene thiophene and furan derivatives deposited on a gold colloidal surface. *J. Mol. Struct*. **2016**, 1122, 198–204.

30. Garrido C., Aliaga A.E., Gomez-Jeria J.S., Clavijo R.E., Campos-Vallette M.M. and Sanchez-Cortes S. Adsorption of oligopeptides on silver nanoparticles: surface-enhanced Raman scattering and theoretical studies. *J. Raman Spectrosc*. **2010**, 41(10), 1149-1155.

31. Herrera M.A., Jara G.P., Aliaga A.E., Gómez J.S., Clavijo E., Garrido C., Aguayo T. and Campos Vallette M.M. Surface enhanced Raman scattering study of the antioxidant alkaloid boldine using prismatic silver nanoparticles. *Spectrochim. Acta A* **2014**, 133, 591-596.

32. Garrido C., Aguayo T., Clavijo E., Gómez-Jeria J.S. and Campos-Vallette M.M. The effect of the pH on the interaction of L-arginine with colloidal silver nanoparticles. A Raman and SERS study. *J. Raman Spectrosc.* **2013**, 44 (8) 1105-1110.

33. Aguayo T., Garrido L. C., Clavijo R.E., Gómez-Jeria J.S., Araya M. C., Icaza T.M., Espinoza F. and Campos Vallette M.M. Raman and surface enhanced Raman scattering of a black dyed silk. *J. Raman Spectrosc*. **2013**, 44(9), 1238-1245.

34. Socrates G., *Infrared and Raman Characteristic Group Frequencies, Tables and Charts*, John Wiley & Sons, Chichester, 2001.

35. Lin-Vien D., Colthup N.B., Fateley W.G. and Graselli J.G. *The Handbook of Infrared and Raman Characteristic Frequencies of Organic Molecules*, Academic Press, Boston, 1991.

36. Abdullah, H.H. Kubba R.M. and Shanshal M. Vibration Frequencies Shifts of Naphthalene and Anthracene as Caused by Different Molecular Charges. *Z. Naturforsch.* **2003**, 58a, 645-655.

37. Baran A., Fiedler A., Schulz H. and Baranska M. *In situ* Raman and IR spectroscopic analysis of indigo dye. *Anal. Methods* 2010, **2,** 1372-1376.

38. Kurouski D., Zaleski S., Casadio F., Van Duyne R.P. and Shah N.C. Tip-Enhanced Raman Spectroscopy (TERS) for *in Situ* Identification of Indigo and Iron Gall Ink on Paper. *J. Am. Chem. Soc.* 2014, 136(34), 8677-8684.

39. Moskovits M. Surface-enhanced spectroscopy. *Rev. Mod. Phys.* 1985, 5, 783-826.

40. Aroca R.F., Teo G.Y., Mohan H., Guerrero A.R., Albella P. and Moreno F. Plasmon-Enhanced Fluorescence and Spectral Modification in SHINEF. *J. Phys. Chem. C* 2011, 115(42), 20419-20424.

Table 1. Raman, Surface Enhanced Raman Scattering and Shell-Isolated Nanoparticles Enhanced Raman Scattering peak position of indigo and the most probable vibration mode assignments.

| **Raman Position peak ($cm^{-1}$)** | **SERS[(a)] Position peak ($cm^{-1}$)** | **SHINERS[(b)] Position peak ($cm^{-1}$)** | **Assignment** |
|---|---|---|---|
| 1573 vs[(c)] | 1564 vs | 1581 vs | C=C/C=O str., NH def. [(a)] |
| 1483 mw | 1487 bw | | CH def. |
| 1461 m | 1433 w | | CH def. |
| 1311 m | 1309 wm | 1315 m | ring6 str., def. |
| 1248 w | | 1247 m | CH def. |
| 1225 m | 1194 w | 1225 w | NH def. |
| | 1057 bw | 1049 bm | ring5 str. + $\rho$CO |
| 1015 w | 1018 m | | ring6/ring5 str., def. |
| 859 dvw | | 863 vw | ring6/ring5 str., def. |
| 758 bw | | 757 bm | ring6/ring5 def. |
| 674 mw | | 673 m | ring6/ring5 def. |
| 635 bm | 651 bm | 643 vw | NCC def. |
| 598 m | | 597 m | NH def. |
| | 460 wm | | CNC def. |
| | 401 m | | skel def. |

[(a)]SERS: Surface Enhanced Raman Scattering and

[(b)] SHINERS: Shell-Isolated Nanoparticles Enhanced Raman

[(c)]Symbols and abbreviations: vw, very weak; w, weak; m, medium; s, strong; vs, very strong; d, double; b, broad; sh, shoulder; str. stretching; def., deformation; breath., breathing; skel. skeletal; ring5, ring6, five and six-member rings.

Figure 1.

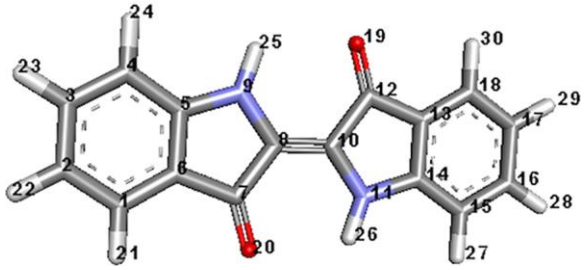

Figure 2.

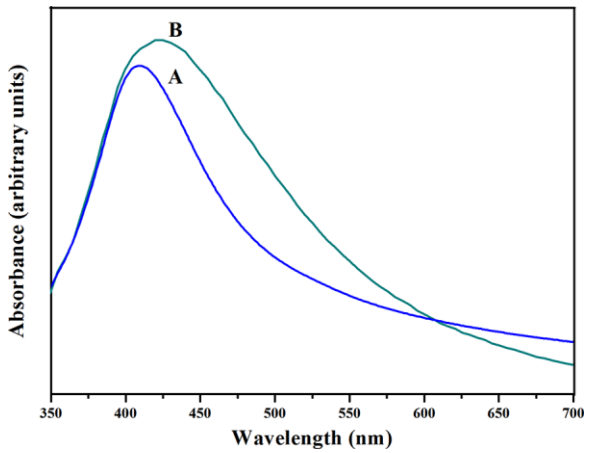

Figure 3.

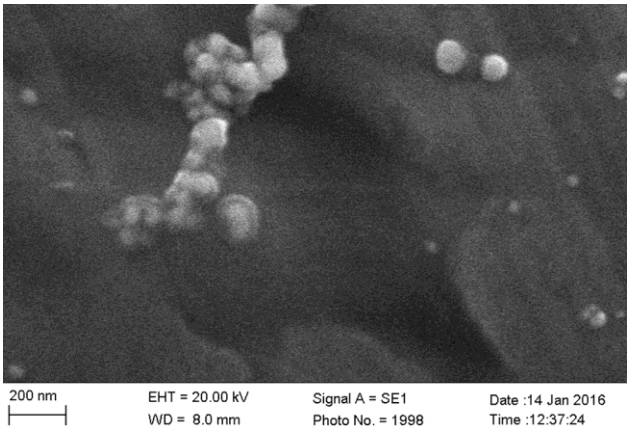

Figure 4.

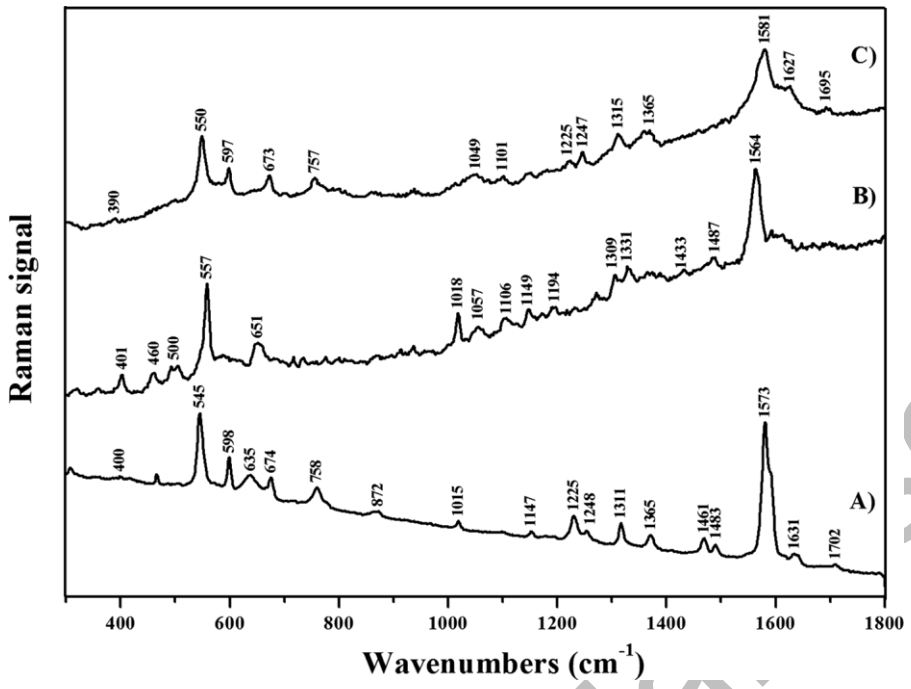

Figure 5.